

Seismic loss-of-support conditions of frictional beam-to-column connections

Cristoforo Demartino^{*1,2}, Giorgio Monti^{1,2a} and Ivo Vanzi^{3,4b}

¹College of Civil Engineering, Nanjing Technical University, Nanjing 211816, PR China

²DISG, Sapienza University of Rome, via A. Gramsci 53, 00197 Rome, Italy

³Department of Engineering and Geology, University "G. d'Annunzio" of Chieti-Pescara, viale Pindaro, 42 65127 Pescara, Italy

⁴College of Civil Engineering, Fuzhou University, Fuzhou, 350108 Fujian, China

(Received June 4, 2016, Revised October 22, 2016, Accepted January 5, 2017)

Abstract. The evaluation of the loss-of-support conditions of frictional beam-to-column connections using simplified numerical models describing the transverse response of a portal-like structure is presented in this paper considering the effects of the seismic-hazard disaggregation. Real earthquake time histories selected from European Strong-motion Database (ESD) are used to show the effects of the seismic-hazard disaggregation on the beam loss-of-support conditions. Seismic events are classified according to different values of magnitudes, epicentral distances and soil conditions (stiff or soft soil) highlighting the importance of considering the characteristics of the seismic input in the assessment of the loss-of-support conditions of frictional beam-to-column connections. A rigid and an elastic model of a frame of a precast industrial building (2-DoF portal-like model) are presented and adopted to find the minimum required friction coefficient to avoid sliding. Then, the mean value of the minimum required friction coefficient with an epicentral distance bin of 10 km is calculated and fitted with a linear function depending on the logarithm of the epicentral distance. A complete parametric analysis varying the horizontal and vertical period of vibration of the structure is performed. Results show that the loss-of-support condition is strongly influenced by magnitude, epicentral distance and soil conditions determining the frequency content of the earthquake time histories and the correlation between the maxima of the horizontal and vertical components. Moreover, as expected, dynamic characteristics of the structure have also a strong influence. Finally, the effect of the column nonlinear behavior (i.e. formation of plastic hinges at the base) is analyzed showing that the connection and the column are a series system where the maximum force is limited by the element having the minimum strength. Two different longitudinal reinforcement ratios are analyzed demonstrating that the column strength variation changes the system response.

Keywords: loss of support; disaggregation; friction coefficient; precast industrial buildings; beam-to-column connections

1. Introduction

Single story precast industrial buildings are widely used for their fast construction time and relatively low construction costs. Moreover, this structural typology guarantees standardization of spatial organization and structural layouts permitting a substantial reduction in the number of standard sizes for components and structural members. Nowadays, with reference to Europe, one-story industrial precast concrete buildings are the most common type to be found at industrial enterprises and constitute 75÷80% of total industrial construction. Precast industrial buildings are very efficient under dead and wind loads. Differently, in the case of seismic events with strong horizontal and vertical actions, they show all their vulnerabilities. These structural deficiencies referring to all

the structural and non-structural elements were observed during the recent devastating earthquakes in China (2008 and 2010), New Zealand (2011), Japan (2011), Turkey (2011) and Italy (2009 and 2012). The main problem of these structures is related to the inefficient mechanical behavior of beam-to-column connections in which the shear transfer usually relies on friction.

A precast structure is an assemblage of precast elements which, when suitably connected together, form a 3D framework capable of resisting to the dead and live load (Elliott 2002). The typical structure used as industrial building is a single story frame (Sezen *et al.* 2000, Dassori and Assobeton 2001, Posada and Wood 2002, Zhu *et al.* 2015) composed of precast concrete elements (Fig. 1): two foundation systems, two columns and one beam. Considering non-seismic designed structures, the columns cross-section is relatively small and in this case the foundation is usually realized using precast socket foundations. The columns are modeled as base-fixed cantilever columns (inserted in precast socket footings) with precast beams placed on top of them featuring simple supported behavior loading roof systems of different typologies. In both precast columns and beams, concrete is of the highest quality due to their production and casting in a controlled environment. The beam supports the roof

*Corresponding author, Ph.D.

E-mail: cristoforo.demartino@uniroma1.it

^aProfessor

E-mail: giorgio.monti@uniroma1.it

^bProfessor

E-mail: i.vanzi@unich.it

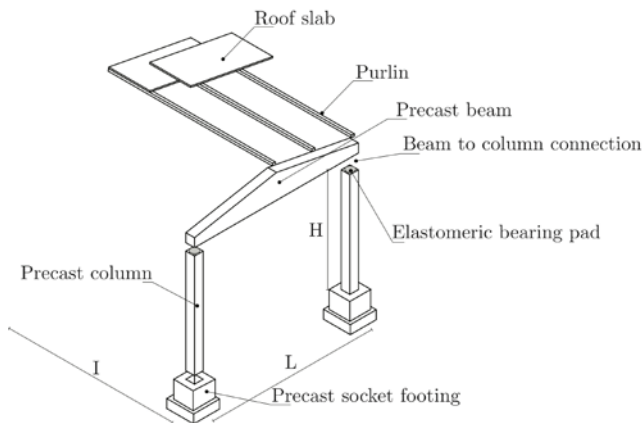


Fig. 1 Precast industrial building structure

system that is usually made with secondary beams (purlins) supporting roof slabs and/or roof windows. One-story industrial buildings were characterized by long-span roof beams, which provided large open areas needed for manufacturing (Dassori and Assobeton 2001). The buildings are usually rectangular. Transverse bay widths usually range from $L=10$ to 30 m, and longitudinal bay widths (frame spacing) ranges from $I=6$ to 14 m and story heights also range from $H=4$ to 9 m.

The main difference between a normal concrete structure and a precast one is the presence of joints that strongly affect the mechanical behavior. In fact, this type of buildings is usually made by the superposition (i.e., joining) of structural elements to obtain precast portal frames. In many countries (USA, New Zealand, Japan, Australia, etc.), rigid connections are preferred for beam-column joints, while in Europe (Italy, Greece, Spain, Portugal, Slovenia, etc.) and elsewhere (Turkey, Armenia etc.), simple dry pinned connections are traditionally used in frame type buildings (Psycharis and Mouzakis 2012). Beam-to-column joints are built with many technologies (Elliott and Jolly 2013): (i) dry bearing of precast to precast, (ii) extended bearings where the temporary bearing is small and reinforced in-situ concrete is used to complete the connection, (iii) dry-packed bearing, where components are located on thin (3 to 10 mm thick) shims and the resulting small gap is filled using semi-dry sand/cement grout, (iv) bedded bearing, where components are positioned onto a prepared semi-wet sand/cement grout, (v) elastomeric or soft bearing using neoprene rubber or similar bearing pads and (vi) steel bearing using steel plates or structural steel sections. An example of connection realized using an elastomeric beam pad is reported in Fig. 1.

In this study, attention will be paid to non-seismic designed structures in which the shear transfer mechanism in the beam-to-column connection mainly relies on friction. Generally, in non-seismic designed single story industrial precast buildings, beam-to-column dry pinned connections are employed in which a dowel is often added more with the purpose of centering column and beam during the assembling leaving the shear forces transfer mechanism mainly based on the friction between the contact surfaces. The friction coefficients reported in literature are characterized by large variability of the data; in general, it

can be assumed that for concrete-to-concrete surfaces the friction coefficient ranges from 0.5 to 1.2 mainly depending on the roughness of the surfaces and on the normal tension (Mohamad *et al.* 2015) while for neoprene-to-concrete it ranges from 0.1 to 0.5 mainly depending on normal tension (Magliulo *et al.* 2011).

Different authors tried to characterize the loss-of-support conditions. Magliulo *et al.* (2014), Belleri *et al.* (2014) evaluated the minimum required friction coefficient to avoid sliding in the hypothesis of perfect correlation between the maxima of the vertical and horizontal components of the earthquake input. However, they used a very limited set of earthquake data, only 1 strong-motion time history (20 May 2012 recorded in Mirandola station-MRN according to the nomenclature of the Italian Rete Accelerometrica Nazionale (RAN) network (DPC 2016)). Only Belleri *et al.* (2014) included the effects of the vertical components of the seismic input in their calculations. Casotto *et al.* (2015) presented a seismic fragility model for Italian RC precast buildings, to be used in earthquake loss estimation and seismic risk assessment. The collapse limit state is related to the beam loss of support or with the complete damage of the columns. They executed nonlinear dynamic analyses and the loss of support of the beam was defined in two ways: (i) when the shear demand in at least one column exceeds the connection capacity computed assuming a constant vertical force with a friction coefficient of 0.4; (ii) when the sliding displacement of the beam calculated using the Newmark sliding block analysis (Kramer 1996) exceeds its support length considering the capacity dependent on the vertical component of the ground motion records. Similarly, Babič and Dolšek (2016) derived fragility functions of 12 classes of Italian precast buildings and presented for two types of intensity measures (peak ground accelerations and spectral accelerations) and for five different damage states considering the effects of non-structural components such as vertical and horizontal panels and infill elements. However, although different models and framework for the fragility evaluation were derived and the risk associated to beam unseating was demonstrated, little attention has been paid to the evaluation of the effects of the seismic-hazard disaggregation on the loss-of-support conditions of frictional beam-to-column connections and to the evaluation of the minimum required friction coefficient to avoid sliding using a large set of strong-motion inputs.

This paper addresses the evaluation of the loss-of-support conditions of frictional beam-to-column connections using simplified numerical models describing the transverse response of a portal-like structure considering the effects of the seismic-hazard disaggregation. In Section 2, real earthquake time histories selected from European Strong-motion Database (ESD) are classified according to different values of magnitude, epicentral distance and soil conditions (stiff or soft soil) highlighting the importance of considering the characteristics of the seismic input in the assessment of frictional beam-to-column connections. A rigid (Section 3) and an elastic (Section 4) model of a frame of a precast industrial building (portal-like model) are presented and adopted to find the minimum required friction coefficient to avoid sliding. Then, the mean value of the minimum required friction coefficient with an epicentral

Table 1 Summary of the subset characteristics. Ground type is classified according to EuroCode 8 (CEN 2004)

Subset	Name of the subset	Magnitude	$V_{s,30}$ (Ground type)	N° records	d
1	Low magnitude -stiff soil	$4 < \text{Magnitude} < 5.5$	< 360 m/s (A and B)	483	< 70 km
2	High magnitude -stiff soil	$5.5 < \text{Magnitude} < 7$	< 360 m/s (A and B)	283	< 70 km
3	Low magnitude -soft soil	$4 < \text{Magnitude} < 5.5$	> 360 m/s (B and C)	135	< 70 km
4	High magnitude -soft soil	$5.5 < \text{Magnitude} < 7$	< 360 m/s (B and C)	77	< 70 km

distance bin of 10 km is calculated and fitted with a linear function depending on the logarithm of the epicentral distance. In Subsection 4.1, a complete parametric analysis varying the horizontal and vertical period of vibration of the structure is performed. In Section 5, the effect of the columns nonlinear behavior is analyzed showing that the connection and the column are a series system where the maximum force is limited by the element having the minimum strength. Two different longitudinal reinforcement ratios are analyzed demonstrating that the column strength variation changes the system response. Finally, some conclusions and prospects are drawn (Section 6).

2. Strong-motion database: characteristics and record processing

A comprehensive database from the European Strong-motion Database (ESD) of accelerograms recorded between 1970 and 2008 (Ambraseys *et al.* 2004) was used in the analyses. ESD contains 2,213 strong-motion records obtained from 856 earthquakes recorded at 691 different stations. The strong-motion records are reported with all the three components: two mutually perpendicular horizontal components, $a_{h,i}(t)$, and a vertical component, $a_v(t)$. The subscript $i = \{NS, EW\}$ indicates that the horizontal component of the strong-motion records is related to two possible horizontal directions: North-South and East-West.

ESD classified the strong-motion records with different parameters. First, parameters that characterize the source are given: magnitude (moment magnitude scale from 4 to 8), the date and origin time, hypocentral location and fault mechanism. Moreover, ESD contains information on the stations, which recorded strong-motion data: location, altitude and local site conditions. The epicentral distance, d , is calculated using the previous information (i.e. location of the station and of the epicenter). Station local soil conditions are classified according to the classification of EuroCode 8 (CEN 2004) (same of the Italian Building Code (MIT 2008)) using the value of the shear wave velocity value averaged over the upper 30 m of the site, $V_{s,30}$, into 4 site categories: very soft soil (Ground type D - $V_{s,30} < 180$ m/s), soft soil (Ground type C - $180 \text{ m/s} \leq V_{s,30} < 360$ m/s), stiff soil (Ground type B - $360 \text{ m/s} \leq V_{s,30} < 750$ m/s) and rock (Ground type A - $V_{s,30} \geq 750$ m/s). This classification was made using shear-wave velocity profiles if available or other information if these profiles are not available

(Ambraseys *et al.* 2004).

The strong-motion records were divided into 4 subsets with characteristics reported in Table 1. In particular, ESD strong-motion records were classified using two magnitude ranges and two ground types (i.e., ground types A and B and ground types C and D). All the fault mechanism and hypocentral location are considered in each subset. Because the objective of this study is to investigate the effects of the seismic-hazard disaggregation on the loss-of-support conditions of frictional beam-to-column connections, strong-motion records with epicentral distances larger than 70 km were disregarded as not enough intense to produce sliding in the connection for actual values of the friction coefficient. All of the selected recordings come from a free-field site. The range of the parameters defining the subsets is chosen in order to balance the needs to have a sufficiently large number of strong-motion records and to reduce the seismic input variability. Operating in this way, a total of 766 strong-motion records were selected for the subsets 1 and 2, i.e., stiff soil, and 212 recordings for the subsets 3 and 4, i.e., soft soil. The number of strong-motion records for each subset is reported in Table 1. Finally, each of the 4 subsets is divided into 7 sub-subsets characterized by epicentral distance bins from 0 to 70 km with steps of 10 km; this is done as in the following all the evaluated parameters will be averaged in each sub-subset.

The distribution of the records with respect to the epicentral distance (i.e., to the sub-subsets) is shown in Fig. 2 for the 4 subsets. For low magnitude cases (blue bars), most of the strong-motion records are at an epicentral distance smaller than 30 km and the largest number was found at 20 km. Differently, for the high magnitude cases

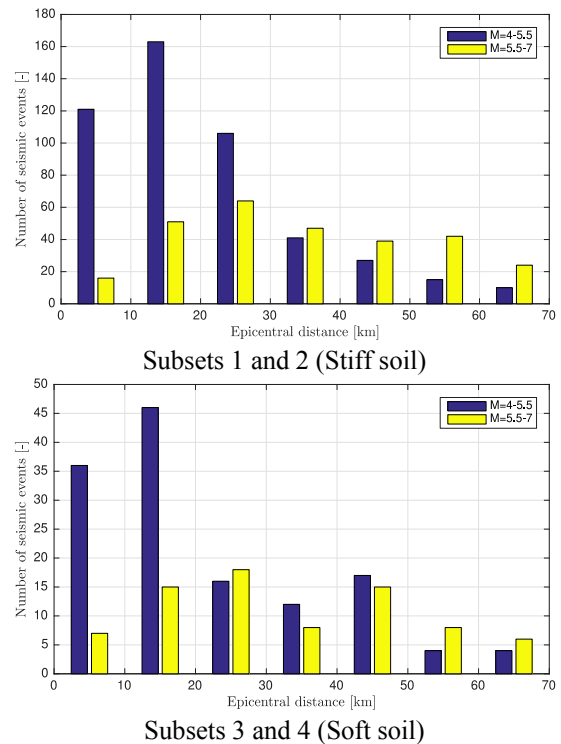


Fig. 2 Histogram of the seismic events as a function of the epicentral distance (sub-subsets) for the 4 subsets

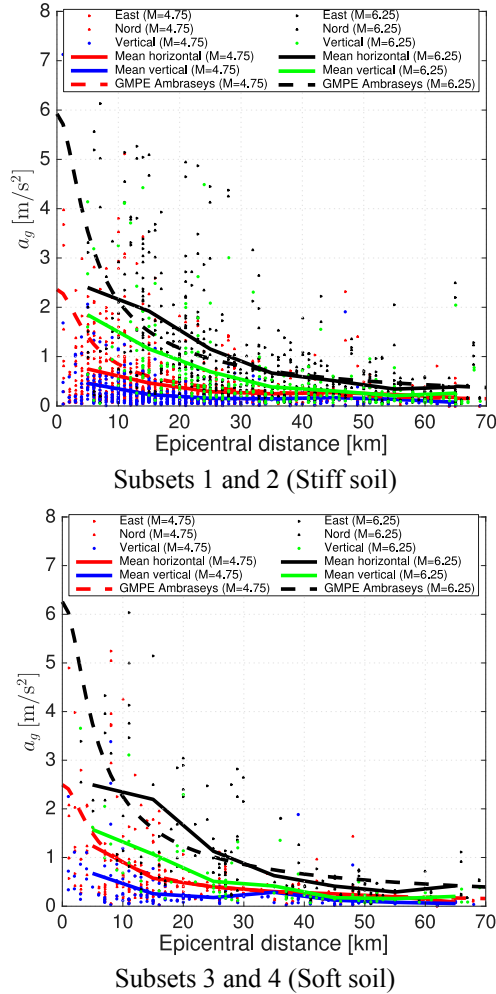


Fig. 3 Peak ground acceleration, a_g , for the three mutual directions as a function of the epicentral distance for the 4 subsets

(yellow bars) most of the strong-motion records are at an epicentral distance from 20 km to 60 km with the minimum number of strong-motion records at 10 km and 70 km. The minimum number of records in each sub-subset is 4 for low magnitude cases and 6 for high magnitude cases: both values are larger than the minimum number reported in EuroCode 8 (CEN 2004) that established that the suite of recorded accelerograms to be used should consist of a minimum of 3 accelerograms.

In Fig. 3 the peak ground acceleration, a_g , for the three mutual directions is reported as a function of the epicentral distance for the 4 subsets. In this context, the mean is the average of the data with a bin of 10 km (i.e., in each sub-subset) and the horizontal direction is mean of the two horizontal components; this is in agreement with the common definition of the Ground-Motion Prediction Equation (GMPE) (e.g., Barani *et al.* 2015). As expected, the mean in the horizontal and vertical directions decreases with the epicentral distance.

In order to validate the 4 subsets of records, these were compared with the GMPE of Ambraseys *et al.* (1996). This GMPE is chosen as it was derived using earthquakes of the European area. The GMPE has the following expression

(Ambraseys *et al.* 1996)

$$\log(a_g) = -1.48 + 0.226 \cdot M_S - 0.922 \cdot \left(\sqrt{d^2 + h_0^2} \right) + 0.117 \cdot S_A + 0.124 \cdot S_S \quad (1)$$

where M_S is the surface wave magnitude (i.e., the mean value of the subset range of magnitude reported in Table 1 converted using the relationship of Yenier *et al.* (2008)), d is the epicentral distance expressed in km, $h_0=3.5$ km accounts for the fact that the source of the peak motion is not necessarily the closest point on the surface projection of the fault, or from the epicenter, and it does not represent explicitly the effect of the depth on the acceleration (Ambraseys *et al.* 1996) and S_A is a coefficient that takes the value of 1 if the site is classified as stiff and 0 otherwise, and S_S is defined in the same way for soft soil sites. The comparison shows the good agreement between the mean of the horizontal direction and the GMPE of Ambraseys *et al.* (1996) for all the four subsets of strong-motion records. Similar considerations were obtained for the maximum spectral acceleration values and associated period, although these results are not reported for the sake of brevity.

2. Rigid block model

In this Section, an unrestrained rigid block model is presented. Similar models were adopted in many studies considering only the horizontal component (e.g., Pompei *et al.* 1998) and also the vertical component (e.g., Taniguchi 2002). However, Lopez Garcia and Soong (2003a, b) found that without taking into account vertical base accelerations the sliding prediction could be significantly unconservative, especially for relatively large values of the friction coefficient. Rigid block models are employed in the evaluation of non-structural components such as building contents and mechanical/electrical equipment whose behavior is essentially that of a rigid body (Lopez Garcia and Soong 2003a, b). Even though these models are not appropriate for the evaluation of the seismic response of frictional beam-to-column connections, these are presented and adopted in the following for completeness as they are the limiting cases of infinitive horizontal and vertical stiffness of the portal-like elastic model (Section 4).

Generally speaking, the responses of a rigid body can be classified into two initial responses (liftoff and slip) and four subsequent responses (Taniguchi 2002): (i) pure liftoff motion, (ii) liftoff-slip interaction motion, (iii) pure slip motion and (iv) slip-liftoff interaction motion. The rigid block model considered in this Section is shown in Figure 4, where a rigid block of mass M rests on a frictional device with friction coefficient $\bar{\mu}$, representing the interface conditions. Only the pure slip motion is considered, i.e., only horizontal translation of the body; accordingly, the frictional device allows only the horizontal motion, $x_{h,i}(t)$. The block is subjected to the gravity load, $M \cdot g$, and to horizontal and vertical base excitations $a_{h,i}(t)$ and $a_v(t)$, respectively. The only resistance to horizontal inertia force is the friction force, $F_{f,i}(t)$. The Equation of Motion (EoM) of the rigid block model

$$M \cdot a_{h,i}(t) = F_{f,i}(t) \quad (2)$$

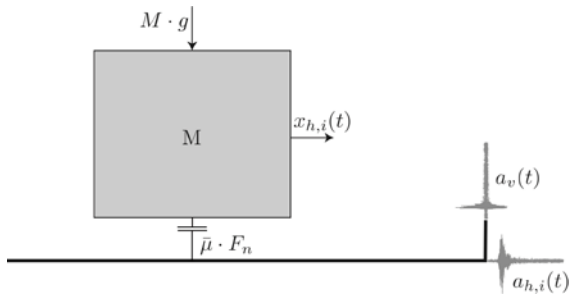


Fig. 4 Rigid block model

where, assuming a Coulomb-type friction model, the friction force is

$$F_{f,i}(t) = \begin{cases} M \cdot a_{h,i}(t) & \text{if } M \cdot a_{h,i}(t) \leq \bar{\mu} F_n(t) \\ \bar{\mu} F_n(t) & \text{if } M \cdot a_{h,i}(t) > \bar{\mu} F_n(t) \end{cases} \quad (3)$$

where $F_n(t) = M(g + a_v(t))$. The subscripts v and $i = \{NS, EW\}$ indicate that the variable is related to the vertical and horizontal (North-South and East-West) direction, respectively.

Eq. (3) defines two distinct behaviors: (i) non-slip mode with non-relative displacements between the block and the horizontal supporting surface and (ii) slip mode with relative displacements. The non-sliding condition at time t occurs when the capacity of the connection, $F_{f,i}(t)$, is greater than the demand, $M \cdot a_{h,i}(t)$; this is used to find the following condition for the minimum required friction coefficient to avoid sliding

$$\mu_i = \max_t \frac{|a_{h,i}(t)|}{g + a_v(t)} \quad (4)$$

If $g + a_v(t)$ is negative, uplift conditions occur and it is not possible to find a minimum required friction coefficient to avoid sliding (as negative solutions of μ_i are without physical meaning).

The minimum required friction coefficient is computed for the two horizontal directions North-South and East-West and the maximum is calculated as

$$\mu = \max_i \mu_i \quad (5)$$

μ for a rigid block can be related to the vertical-to-horizontal response ratio, V/H , adopted by many authors to define the vertical action (e.g., Bozorgnia and Campbell 2004, Gülerce and Abrahamson 2011, Bommer *et al.* 2011). In particular, assuming that the maxima of the horizontal and vertical component are simultaneous, Eq. (4) can be rearranged to express the minimum required friction coefficient as a function of V/H

$$\mu = \max_i \left(\frac{g}{\max_t a_{h,i}(t)} \pm \frac{\max_t a_v(t)}{\max_t a_{h,i}(t)} \right)^{-1} = \left(\frac{g}{\max_t a_{h,i}(t)} \pm V/H \right)^{-1} \quad (6)$$

where the two solutions, with the plus and the minus sign, represent the upper-bound and the lower-bound of the solution, i.e., maximum of the horizontal component combined simultaneously with positive or negative maximum value of the vertical component, respectively.

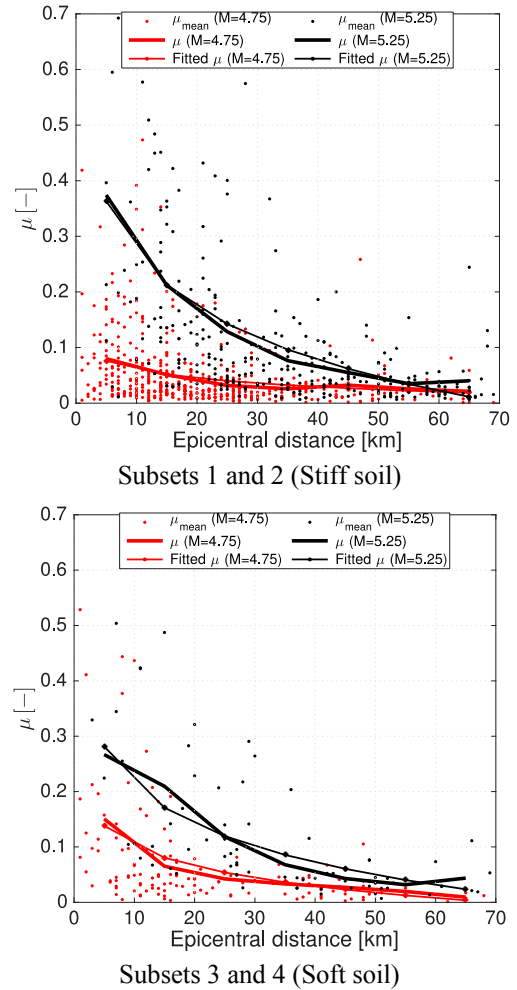


Fig. 5 μ (Eq. (5)) and its mean value, μ_{mean} , as a function of the epicentral distance for the 4 subsets. Fitted values of μ_{mean} using Eq. (7)

The solution accounting for the real maxima correlation reported in Eq. (4) falls between these two limiting cases. The solution reported in Eq. (6) can be adopted for the evaluation of the minimum required friction coefficient using the GMPEs available for the peak ground acceleration (e.g., Ambraseys *et al.* 1996) and for the V/H coefficient (e.g., Bozorgnia and Campbell 2004, Gülerce and Abrahamson 2011, Bommer *et al.* 2011).

Large values of V/H lead to large differences between the upper bound and the lower bound of the solution (Eq. (6)). Generally, V/H assumes larger values for large magnitudes, close distances and soft soil conditions (Bozorgnia and Campbell 2004). Moreover, V/H can be derived from design codes that usually defines the vertical component of motion in terms of response spectrum simply as $2/3$ (Newmark *et al.* 1973) of the horizontal spectrum at all response periods (Bommer *et al.* 2011) or from Eurocode 8 (CEN 2004) that was among the first codes to include a vertical spectrum defined independently from the horizontal spectrum, based largely on the proposed V/H model of Elnashai and Papazoglou (1997).

In Fig. 5, the minimum required friction coefficient for a rigid block evaluated according to Eq. (5) is reported as a

Table 2 Fitted parameters of $\mu_{mean}(d)$ (Eq. (7)) and R -square values for the 4 subsets

	Stiff soil		Soft soil	
Magnitude	4.75	5.25	4.75	5.25
Subset	1	2	3	4
a [-]	0.1120	0.5837	0.2223	0.4431
b [km^{-1}]	-0.0224	-0.1371	-0.0524	-0.1005
R -square	0.9313	0.9827	0.9540	0.9453

function of the epicentral distance for the 4 subsets. Here and in the following, μ_{mean} is the average of the data with a bin of 10 km (i.e., in each sub-subset). For each subset, μ_{mean} values reported as a function of the logarithm of the epicentral distance were fitted (in a least-squares sense) using the following degree 1 polynomial

$$\mu_{mean}(d) = a + b \cdot \log d \quad (7)$$

where a represent the minimum required friction coefficient at $d=0$ km (i.e., asymptotic value) and b is the slope. Results of the estimation are reported in Fig. 5 and in Table 2. In Fig. 5, it can be seen the good agreement between the fitted polynomial and the μ_{mean} values; this is also confirmed by the values near to the unit of the coefficient of determination (R -square) reported in Table 2. Globally, increasing the magnitude and reducing the epicentral distance, the minimum required friction coefficient increases, according to the increase of the input action (Fig. 3). The maximum required friction coefficient was found for the subset 2 ($a=0.5837$) that also has the maximum slope. Considering the low magnitude events (subsets 1 and 3), the maximum required friction coefficient was found for the subset 3 (0.2223); this is in agreement with the values of the horizontal component of a_g that is larger for subset 3 than for subset 1 (Fig. 3). For epicentral distances lower than about 30 km and high magnitude subsets, a minimum required friction coefficient compatible with the neoprene-concrete contact surfaces, $\mu=0.1-0.3$ (Magliulo *et al.* 2011), was found.

3. Portal-like elastic model

In this Section, a portal-like elastic model is presented. Many authors proposed a similar model to define the transverse response of one frame of a one-story precast industrial building (Fig. 1) modeling with different level of complexity the non-linear behavior of the foundations, of the columns and of the beam-to-column connections (Liberatore *et al.* 2013, Magliulo *et al.* 2014, Casotto *et al.* 2015).

The portal-like elastic model consists of two cantilever columns on top of which is located a simply supported beam considering the beam-to-column connections as hinges with large rotation capacity (Fig. 6(a)). This continuous model can be condensed into a discrete 2 Degrees of Freedom (DoFs) model using the following assumptions: (i) the mass of the columns is neglected, (ii) the mass of the beam and of the roof system is uniformly

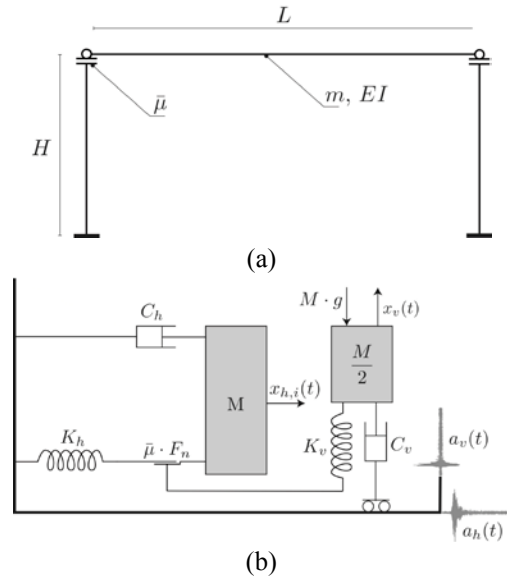


Fig. 6 Portal-like elastic model (a) and mechanical model (b)

distributed on the beam, (iii) the beam cross section is constant, (iv) only the first vertical and horizontal modes of vibrations are considered, (v) the motion of the structure is only in the transverse direction and (vi) the beam and column axial deformability is neglected. Using these assumptions, the structure is reduced into a 2-DoFs elastic model (Fig. 6(b)).

The first DoF is related to the vertical response of the beam while the second DoF is the horizontal response than occurs be in the North-South and East-West directions (according to the ground motion time histories presented in Section 2). The EoMs of the 2-DoFs elastic mechanical model are

$$\begin{aligned} 0.5 \cdot M \ddot{x}_v(t) + C_v \dot{x}_v(t) + K_v x_v(t) &= -0.5 \cdot M a_v(t) - M \cdot g \\ M \ddot{x}_{h,i}(t) + C_h \dot{x}_{h,i}(t) + K_h x_{h,i}(t) &= -M a_{h,i}(t) + F_{f,i}(t) n \end{aligned} \quad (8)$$

where t is the time, M is the lumped mass of the beam and of the roof system, C is the damping coefficient, K is the stiffness, $a(t)$ is the ground-motion time history and assuming a Coulomb-type friction model, the friction force is

$$F_{f,i} = \begin{cases} M \cdot a_{h,i}(t) & \text{if } M \cdot a_{h,i}(t) \leq \bar{\mu} F_n(t) \\ \bar{\mu} F_n(t) & \text{if } M \cdot a_{h,i}(t) > \bar{\mu} F_n(t) \end{cases} \quad (9)$$

where $F_n(t) = M(g + 0.5 \cdot \ddot{x}_v(t))$ is the normal force exerted by each surface on the other in the beam-to-column connections. The subscripts v and $i = \{NS, EW\}$ indicate that the variable is related to the vertical and horizontal (North-South and East-West) direction, respectively.

In Eq. (8) in the vertical direction, the mass multiplier 0.5 transform the total mass into the first modal mass of a simple supported beam

$$M_v = \int_0^L m \phi_1^2(x) dx = \int_0^L m \sin^2\left(\frac{\pi}{L} x\right) dx = 0.5 M \quad (10)$$

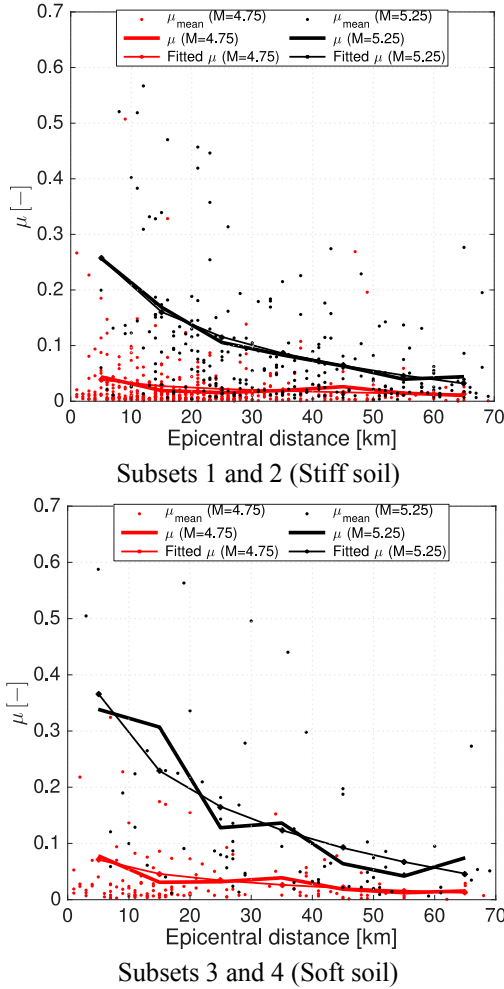


Fig. 7 μ (Eq. (5)) and its mean value, μ_{mean} , as a function of the epicentral distance for the 4 subsets. Fitted values of μ_{mean} using Eq. (7). ($T_v=0.1s$; $T_h=1s$; $\zeta_v=1\%$; $\zeta_h=3\%$)

The natural periods of the vertical and horizontal DoFs are equal to

$$T_v = 2\pi \cdot \sqrt{\frac{0.5 \cdot M}{K_v}} \quad T_h = 2\pi \cdot \sqrt{\frac{M}{K_h}} \quad (11)$$

Using the same definitions adopted in the previous section, the minimum required friction coefficient to avoid sliding is

$$\mu_i = \max_t \frac{|\ddot{x}_{h,d}(t)|}{g + 0.5 \cdot \ddot{x}_v(t)} \quad (12)$$

If $g + 0.5 \cdot \ddot{x}_v(t)$ is negative, uplift conditions occur. Finally, the maximum for the two horizontal directions North-South and East-West is calculated as

$$\mu = \max_i \mu_i \quad (13)$$

It should be highlighted that μ depends on different parameters: (i) T_v , (ii) T_h , (iii) C_h , (iv) C_v and (v) sub-subset (i.e., epicentral distance, magnitude and ground type).

In the following, results of the analyses performed considering a specific industrial precast building with

Table 3 Fitted parameters of $\mu_{mean}(d)$ (Eq. (7)) and R -square values for the 4 subsets. ($T_v=0.1s$; $T_h=1s$; $\zeta_v=1\%$; $\zeta_h=3\%$)

	Stiff soil		Soft soil	
Magnitude	4.75	5.25	4.75	5.25
Subset	1	2	3	4
a [-]	0.0547	0.3984	0.1082	0.5674
b [km^{-1}]	-0.0102	-0.0878	-0.0230	-0.1248
R-square	0.6715	0.9897	0.8456	0.8759

common characteristics ($T_v=0.1s$; $T_h=1s$; $\zeta_v=1\%$; $\zeta_h=3\%$) are presented. The natural periods were chosen in order to obtain dynamic characteristics of typical Italian precast industrial building calculated using their mean geometric characteristics (e.g., Bellotti *et al.* 2014) and the damping coefficient are representing of possible low values evaluated using a reasonable engineering judgment criteria. As a matter of fact, to the best authors' knowledge, the actual structural damping coefficient of operating industrial precast building are not available into the literature and/or public domain information.

In Fig. 7, the minimum required friction coefficient for a portal-like model evaluated according to Eq. (13) is reported as a function of the epicentral distance for the 4 subsets. For each subset, μ_{mean} values reported as a function of the logarithm of the epicentral distance were fitted (in a least-squares sense) using Eq. (7) and results of the estimation are reported in Fig. 7 and in Table 3.

The coefficient of determination (R -square) reported in Table 3 is lower (except for the subset 2) compared with the rigid block model (Table 2), although the fitting can be considered acceptable. In this case, the minimum required friction coefficient at zero epicentral distance, a , is smaller for low magnitude subsets compared with the rigid block model. Differently, for high magnitude subsets, a is larger for soft soil and smaller for stiff soil compared with the rigid block model. In this case, for the soft soil subsets, a is larger than those of the stiff soil subsets. This is due to the different spectral content at these structural natural periods of both vertical and horizontal strong motion input. Finally, it should be highlighted that between the two models the vertical mass is different: M for the rigid model and $0.5M$ for the portal-like elastic model. This makes the results not directly comparable as in the portal-like elastic model the effect of the vertical motion is filtered by the beam dynamics.

The slope, b , of the low magnitude events, is approximately equal to 0 km^{-1} indicating roughly constant values of μ varying d . On the other hand, for high magnitude subsets b assumes larger negative values (comparable with the rigid block case) indicating marked decreasing of μ varying d . Also in this case, for epicentral distances lower than about 30 km and high magnitude subsets, a minimum required friction coefficient compatible with the neoprene-concrete contact surfaces (Magliulo *et al.* 2011) was found. Differently, for low magnitude subsets, μ is lower than the friction coefficient of neoprene-concrete contact surfaces indicating no susceptibility to sliding for the beam-to-column connections if the sliding connection

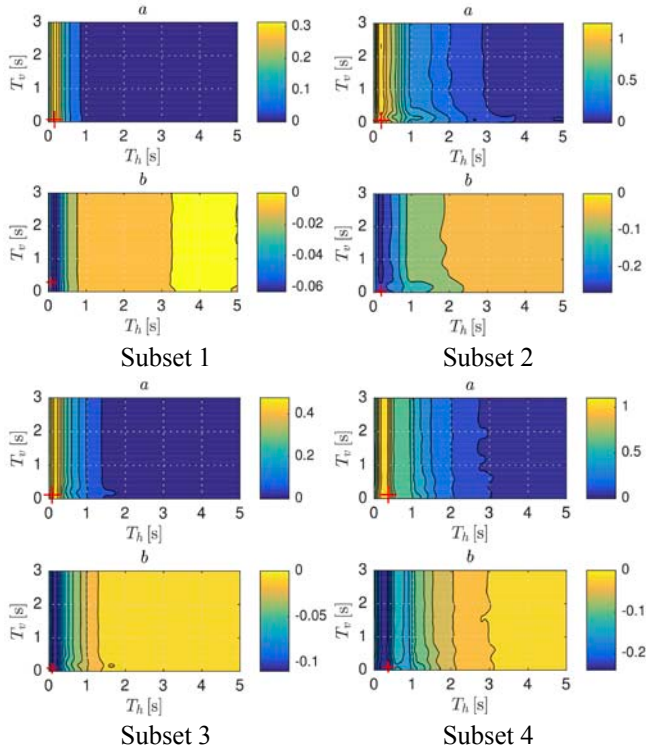


Fig. 8 Contour plot of a and b (Eq. (7)) in the T_h - T_v plane for the 4 subsets. The red plus sign indicates the T_h - T_v coordinates of the absolute maximum value. ($\zeta_v=1\%$; $\zeta_h=3\%$)

mechanism is the weakest. In the following Section, a simplified method to account for the column nonlinear behavior will be given.

4.1 Parametric study of the horizontal and vertical natural periods

The results reported in Fig. 7 and in Table 3 were evaluated using the dynamic characteristics of a specific building ($T_v=0.1$ s; $T_h=1$ s; $\zeta_v=1\%$; $\zeta_h=3\%$). In order to shed light on the variability of $\mu_{mean}(d)$ with T_v and T_h , the fitted parameters of $\mu_{mean}(d)$ using Eq. (7) were evaluated for different values of T_v (range and step: 0:0.05:3 s) and T_h (range and step: 0:0.05:5 s) having fixed the structural damping as in the previous case ($\zeta_v=1\%$; $\zeta_h=3\%$); this was done for all the four subsets. For a fundamental period equal to 0 s the solution of $\mu_{mean}(d)$ reported in Section 3 was adopted while for the other cases those reported in Section 4. In order to simplify the comparison, for both rigid and portal-like elastic model a vertical mass equal to $0.5M$ was adopted. As a matter of fact, in this context, the rigid body solution is only the asymptotic case considering infinite stiffness.

Contour plots of the estimated a and b coefficient in the T_v - T_h plane are reported in Fig. 8; the maximum values of a and the corresponding T_v and T_h values are reported in Table 4 for the 4 subsets. The larger values of a were found for low values of T_h , around 0.2 s, for all the subsets. The vertical component influences a and b for values of T_v smaller than 0.3 s; for T_v larger than this threshold, a and b

Table 4 Maximum values of a (Eq. (7)) and corresponding T_h and T_v values for the 4 subsets. ($\zeta_v=1\%$; $\zeta_h=3\%$)

	Stiff soil		Soft soil	
Magnitude	4.75	5.25	4.75	5.25
Subset	1	2	3	4
max a [-]	0.3555	1.4453	0.5393	1.2614
T_h [s]	0.15	0.20	0.10	0.35
T_v [s]	0.05	0.05	0.10	0.10

depend only on T_h . At low magnitude, the maximum of a was found for soft soil conditions while at high magnitude it was found for stiff soil (Table 4). The subset 4 (high magnitude - stiff soil) shows the wider range of T_h with maximum values of a indicating the large frequency content of the input signal.

Finally, it is worth noting that these data can be used to assess the mean required friction coefficient of a portal-like elastic structure using the dynamic information (T_v , T_h , ζ_v , ζ_h). These can be important for a preliminary assessment of industrial precast structures in order to verify frictional beam-to-column connections.

5. Column nonlinear behaviour

In the previous Sections, an elastic and linear model of the structural behavior was employed. However, during earthquakes, when the horizontal load at the top of the column increases, the cross-section at the base, with the highest bending moment, yields first. At this point, the curvature increases greatly in a limited region located at the base of the column. In these conditions, the base zone is usually modeled as a plastic hinge, i.e., considering all the plastic curvature in a point instead of distributed, and modeling the remaining part of the column as elastic. This mechanical behavior was observed in a large number of precast industrial buildings during the Emilia Romagna earthquakes in Italy in 2012 (ReLUIS *et al.* 2012). In order to consider the columns nonlinear behavior, the full capacity curve of the columns was determined by a quasi-static analysis, i.e., pushover analysis. The analyses reported in the following refer to a typical Italian single story precast industrial building; this is defined as a building having the mean values of the distributions of the characteristics (geometrical and mechanical) reported by Bellotti *et al.* (2014).

A 2D FEM model of one frame of the precast concrete building was built in OpenSees (Version 2.4.6) framework (McKenna *et al.* 2013). The structure is modeled as one frame composed of precast concrete elements made with slender cantilevering columns and simply supported beam (Fig. 6(a)). The columns were modeled using Force-Based Beam-Column Element and the beam using Elastic Beam Column Element. The column and the beam cross-sections are rectangular with base and height equal to 0.5×0.5 m and 0.5×1 m, respectively. The height of the frame is $H=6$ m and the beam length is equal to $L=12$ m. The mass of the roof system is computed considering the specific weight of the beam equal to 2500 kg/m³ and the weight per unit area the roof system equal to 200 kg/m² with a spacing of the frames equal to $I=10$ m, i.e.,

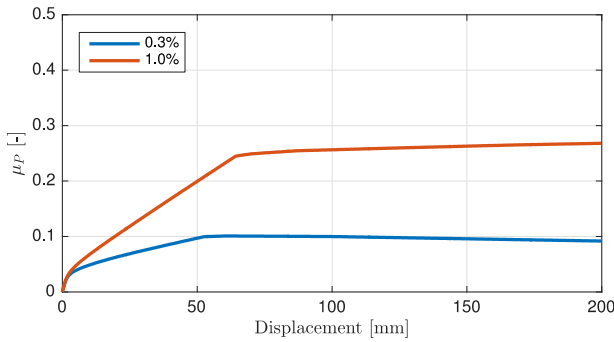


Fig. 9 Pushover curve in terms of μ_p (Eq. (14)) for $\rho_p=0.3\%$ and $\rho_p=1.0\%$

$M=39,000$ kg. The mass of the columns is evaluated considering a density equal to 2500 kg/m^3 .

The properties of concrete and steel are selected following the prescriptions of the Italian building code (MIT 2008) on the base of design values. The concrete adopted in the columns and in the beam is of strength class C45/55 and is characterized by compressive strength f_c equal to 45 MPa, strain corresponding to peak stress is $\varepsilon_y=0.002$, the ultimate strain $\varepsilon_u=0.035$ and tensile strength $f_{ct}=3.8$ MPa. Longitudinal reinforcing steel bars are of type B450C and are characterized by yield stress $f_y=450$ MPa and elastic stiffness $E_s=2.1 \times 10^6$ MPa with a strain-hardening ratio of 0.01. The concrete was modeled using a Concrete02 Material and the steel with a Steel01 Material. In the beam, an elastic material with stiffness equivalent to the concrete was adopted.

Two values of the longitudinal reinforcement ratio were analyzed, i.e., a low one $\rho_p=0.3\%$ (4 Φ 16) and a high one $\rho_p=1.0\%$ (8 Φ 20), being i.e., $\rho_p=A_s/(B_p \cdot H_p)$ with A_s area of the longitudinal steel bars and B_p and H_p base and height of the column cross section. The resulting fundamental periods are $T_h=0.505$ s and $T_v=0.143$ s for $\rho_p=0.3\%$ and $T_h=0.486$ s and $T_v=0.143$ s for $\rho_p=1\%$. The decrease of the horizontal natural periods is due to the increase of the stiffness deriving from the increase of the area of longitudinal steel bars. The structural damping was set as in the previous case, i.e., $\zeta_v=1\%$ and $\zeta_h=3\%$, using a Rayleigh model.

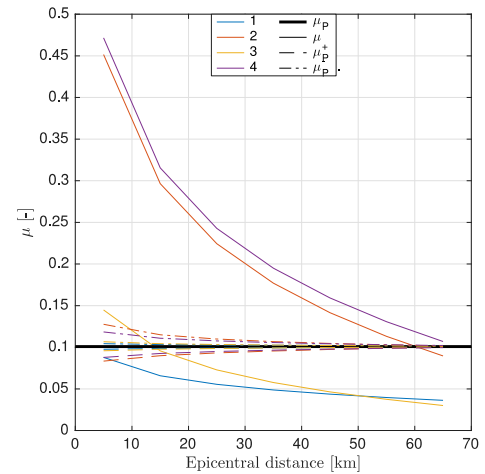
After vertical dead loads application on the structure, one-directional monotonic horizontal displacement-controlled static loading, F_h , was applied on the beam in the range of 0 to 200 mm. Results are shown in Fig. 9 expressed as minimum required friction coefficients to avoid sliding for a given level of column displacement

$$\mu_p = \frac{F_h}{Mg} \quad (14)$$

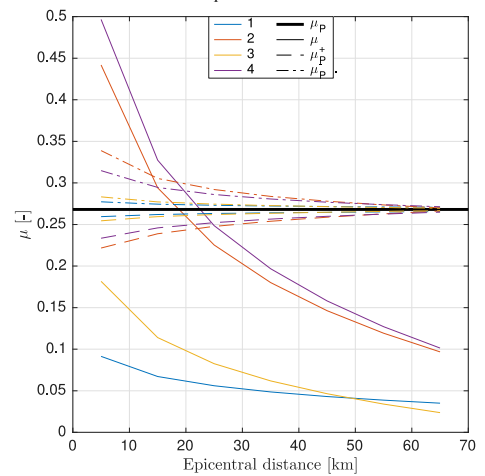
Substituting in Eq. (14) the maximum value of the horizontal force (i.e., column strength), it is found the minimum friction coefficient in the connection required to allow the formation of plastic hinge in the connection

$$\mu_p = \frac{\max F_h}{Mg} = \begin{cases} 0.1 & \text{for } \rho_p=0.3\% \\ 0.27 & \text{for } \rho_p=1.0\% \end{cases} \quad (15)$$

The column and beam-to-column connections are a series system (Fig. 6(b)) and the maximum force is equal to



$\rho_p = 0.3\%$



$\rho_p = 1.0\%$

Fig. 10 μ_p (Eq. (15)), μ (Eq. (13)), μ_p^+ and μ_p^- (Eq. (17)) as a function of the epicentral distance for the 4 subsets. ($\zeta_v=1\%$; $\zeta_h=3\%$)

those of the element characterized by the small strength. Accordingly, the following conditions can occur: (i) $\mu < \mu_p$ and (ii) $\mu \geq \mu_p$. In the first case, the beam-to-column connection sliding is the weakest mechanism and sliding of the connection occur before the formation of the plastic hinges if the friction coefficient in the connection is smaller than μ . In the second case, the formation of the plastic hinge in the columns is the weakest mechanism and sliding condition can occur before of formation of the plastic hinges only if the friction coefficient in the connection is smaller than μ and μ_p . It is worth noting that in both conditions after the activation of the sliding mechanism in the connection or after the formation of the plastic hinges, different mechanisms can occur during the subsequent loading cycles that are characterized by a different behaviour respect to the elastic prediction; this strongly depends on the time-histories characteristics, i.e., duration and intensity of the cycles.

Fig. 10 shows μ_p and μ as a function of the epicentral distance for the 4 subsets and for the two longitudinal reinforcement ratios. The black solid line is the maximum value of the push-over curve reported in Fig. 9 expressed as

(Eq. (15)), μ_p , while the colored solid lines are μ (Eq. (7)) with the coefficients a and b evaluated using the dynamic information (T_v , T_h , ζ_v , ζ_h) of the two analyzed structures, i.e., $\rho_p=0.3\%$ and $\rho_p=1\%$) for the different subsets (i.e., different colors different subsets). In all the cases, μ for soft soil is larger than for stiff soil and assumes slightly larger values for $\rho_p=1\%$.

For $\rho_p=0.3\%$ and low magnitude events (subsets 1 and 3), μ is almost always smaller than μ_p indicating that the weakest mechanism is the sliding in the connection and that if the connection is characterized by a friction coefficient smaller than μ sliding can occur. However, the found values of μ are really low compared with typical values of the friction coefficient of materials employed in beam-to-column connections (e.g., Magliulo *et al.* 2011, Mohamad *et al.* 2015). Values of the friction coefficient larger than μ guarantee an elastic behavior of the structure (i.e., no plastic hinge formation). Only for the subset 3 for epicentral distances smaller than approximately 15 km, the weakest mechanism is the formation of the plastic hinges in the columns. Differently, for $\rho_p=1.0\%$ and low magnitude events (subsets 1 and 3), μ is always smaller than μ_p .

For $\rho_p=0.3\%$ and high magnitude events (subsets 2 and 4), μ is always larger than μ_p , indicating that the weakest mechanism is the formation of the plastic hinges in the columns. Only if the connection is characterized by a friction coefficient smaller than μ_p sliding can occur before the formation of the plastic hinges. For $\rho_p=1.0\%$ and high magnitude events (subsets 2 and 4), μ is almost always smaller than μ_p indicating that the weakest mechanism is the sliding in the connection. Only for epicentral distance smaller than 20 km, μ is larger than μ_p indicating that the weakest mechanism is the formation of the plastic hinges in the columns. Overall, it can be concluded that for the increase of the longitudinal reinforcement ratio leads to an increase of the columns resistance with an increase of the μ_p value.

The definition of μ_p given in Eq. (14) neglects the vertical component effects. In order to account for the vertical component, the maximum spectral vertical acceleration was evaluated for all the strong-motion time histories for each subset. Then, the average of the data with a bin of 10 km (i.e., in each sub-subset) was computed and for each subset mean values, $\max_t \ddot{x}_v(t)_{mean}$, reported as a function of the logarithm of the epicentral distance were fitted (in a least-squares sense) using the following degree 1 polynomial

$$a_v(d) = \left(\max_t \ddot{x}_v(t) \right)_{mean} = a_1 + b_1 \cdot \log d \quad (16)$$

These coefficients were estimated and results are reported in Table 5. It is worth noting that these coefficients assume the same values for the two longitudinal reinforcement ratios adopted as ρ_p has only effects on the horizontal natural periods (i.e., the beam remains the same).

The coefficients a_1 and b_1 (Table 5) can be used to find the upper and lower bound of the minimum required friction coefficients to avoid sliding for a given level of column displacement, μ_p . In particular, considering a perfect correlation between the maximum vertical and horizontal components, the following definition of the

Table 5 Fitted parameters of $a_v(d)$ (Eq. (16)) and R -square for the 4 subsets. ($T_v=0.143$ s; $\zeta_v=1\%$; $\zeta_h=3\%$)

	Stiff soil		Soft soil	
	4.75	5.25	4.75	5.25
Magnitude	1	2	3	4
Subset	1	2	3	4
a_1 [-]	1.8828	13.1778	3.2858	9.1620
b_1 [km^{-1}]	-0.3603	-3.0922	-0.7347	-2.0805
R-square	0.9257	0.9473	0.8730	0.6353

lower and upper bound can be adopted

$$\mu_p^\pm(d) = \frac{\max F_h}{M(g \pm 0.5 \cdot a_v(d))} \quad (17)$$

μ_p^+ and μ_p^- are reported in Fig. 10 as a function of the epicentral distance for the 4 subsets and for the two longitudinal reinforcement ratios. These correspond to the upper and lower bound of the minimum required friction coefficient to avoid sliding in the connection considering the maximum of the horizontal and vertical (positive or negative) components synchronized. It can be seen that the vertical component can lead to a large range of the solution between the upper and lower bounds: the difference between μ_p^+ and μ_p^- increases decreasing the distance due to the increase of the seismic vertical component. For low magnitude events, the larger difference was found for soft soil conditions while for high magnitude events it was found for stiff soil; this is in agreement with the differences observed in a_1 and reported in Table 5. Observing the subset 2 of the $\rho_p=1\%$ case, it can be seen that for epicentral distances in the range of 10 km to 20 km accounting the vertical component makes the lower and upper bounds (orange dashed and dash-dotted lines) of the solution to totally contain μ (orange solid line) inside. This indicates that depending on the degree of correlation of the vertical and horizontal components, the weaker mechanisms can be both the sliding in the connection and the formation of a plastic hinge. However, the limitation of this simple model is to give only the upper and lower bound of the solution. In order to have more detailed information, a complete nonlinear analysis should be performed.

6. Conclusions

This work presented a simple procedure to evaluate the loss-of-support conditions of frictional beam-to-column connections using real earthquake time histories selected from the European Strong-motion Database (ESD). The effects of the seismic-hazard disaggregation were evaluated classifying the ESD seismic events into 4 subsets characterized by two magnitudes (low and high) and two ground types (stiff and soft soil). Moreover, the 4 subsets were divided into 7 sub-subsets characterized by epicentral distance bins from 0 to 70 km with steps of 10 km.

A rigid and an elastic model of a frame of a precast industrial building (2 DoFs portal-like model) were presented and adopted to find the minimum required friction coefficient to avoid sliding. Then, the mean value of

the minimum required friction coefficient with an epicentral distance bin of 10 km was calculated and fitted with a linear function depending on the logarithm of the epicentral distance. The two models were adopted to perform a complete parametric analysis varying the horizontal and vertical period of vibration of the structure in order to derive the two parameters defining the fitted linear function depending on the logarithm of the epicentral distance for all the 4 subsets. The procedure aims to obtain a relationship between the horizontal and vertical periods and the minimum required friction coefficient for different seismic inputs (subsets). These values can be adopted for preliminary evaluation of the risk of loss of support for frictional beam-to-column connection in industrial precast buildings. Results showed that the loss-of-support condition is strongly influenced by magnitude, epicentral distance and soil conditions determining the frequency content of the earthquake time histories and the correlation between the horizontal and vertical components. Moreover, as expected, dynamic characteristics of the structure have also a strong influence. In particular, the larger values of the minimum required friction coefficient required to avoid sliding were found for low values of T_h , around 0.2 s, for all the subsets. The vertical component influences a and b for values of T_v smaller than 0.3 s; for T_v larger than this threshold, a and b depend only on T_h .

Finally, the effect of the columns nonlinear behavior was analyzed showing that the connection and the columns are a series system where the maximum force is limited by the element having the minimum strength. First, the vertical component is neglected and expressing the limit horizontal force in terms of minimum required friction coefficients to avoid sliding for a given level of column displacement, the weakest mechanism between the formation of a plastic hinge and the sliding of the connection was evaluated. Then, considering the vertical and horizontal components of the seismic input perfectly correlated, a simplified procedure for the evaluation of the weakest mechanism was proposed. The output of this model is the upper and lower bound of the minimum required friction coefficients to avoid sliding for a given level of column displacement. The proposed methodology has been applied to a portal-like frame. Two different longitudinal reinforcement ratios were analyzed demonstrating that the column strength variation changes the system response. In particular, the increase of the different longitudinal reinforcement ratio leads to an increase of the columns and to a different definition of the weakest mechanics.

Concluding, it was observed that the seismic input has a strong effect on the minimum required friction coefficient to avoid sliding. On the other hand, it was also shown that linear and non-linear dynamic properties of the structure have a strong effect with either beneficial or detrimental effects. A simplified procedure for the evaluation was proposed. Results provide evidence of the effects of the seismic-hazard disaggregation on the loss-of-support conditions of frictional beam-to-column connections. However, in this study, only the mean values of the minimum required friction coefficient to avoid sliding were evaluated. Future work should, therefore, include the

estimation of the entire probabilistic distribution of the minimum required friction coefficient to avoid sliding. In addition, the final goal should be the implementation of a framework for the risk assessment of loss-of-support conditions of frictional beam-to-column connections considering the seismic-hazard disaggregation at a territorial scale. Further work, currently in progress, is required to investigate these aspects.

Acknowledgments

ReLUIS 2014-2018 project, research line 2.1, is acknowledged for the financial support given to the present research.

References

- Ambraseys, N., Smit, P., Douglas, J., Margaris, B., Sigbjørnsson R., Olafsson, S., Suhadolc, P. and Costa, G. (2004), "Internet site for European strong-motion data", *Bollettino di Geofisica Teorica ed Applicata*, **45**(3), 113-129.
- Ambraseys, N.N., Simpson, K.A. and Bommer, J.J. (1996), "Prediction of horizontal response spectra in Europe", *Earthq. Eng. Struct. Dyn.*, **25**(4), 371-400.
- Babić, A. and Dolšek, M. (2016), "Seismic fragility functions of industrial precast building classes", *Eng. Struct.*, **118**, 357-370.
- Barani, S., Albarello, D., Spallarossa, D. and Massa, M. (2015), "On the influence of horizontal ground-shaking definition on probabilistic seismic-hazard analysis", *Bull. Seismol. Soc. Am.*, **107**(1), doi: 10.1785/0120150033.
- Belleri, A., Brunesi, E., Nascimbene, R., Pagani, M. and Riva, P. (2014), "Seismic performance of precast industrial facilities following major earthquakes in the Italian territory", *J. Perform. Constr. Facil.*, **29**(5), 04014135.
- Bellotti, D., Casotto, C., Crowley, H., Deyanova, M.G., Germagnoli, F., Fianchisti, G., Lucarelli, E., Riva, S. and Nascimbene, R. (2014), "Capannoni monopiano prefabbricati: distribuzione probabilistica dei sistemi e sottosistemi strutturali dagli anni sessanta ad oggi", *Progettazione Sismica*, **5**(3), 41-70.
- Bommer, J.J., Akkar, S. and Kale, O. (2011), "A model for vertical-to-horizontal response spectral ratios for Europe and the Middle East", *Bull. Seismol. Soc. Am.*, **101**(4), 1783-1806.
- Bozorgnia, Y. and Campbell, K.W. (2004), "The vertical-to-horizontal response spectral ratio and tentative procedures for developing simplified V/H and vertical design spectra", *J. Earthq. Eng.*, **8**(2), 175-207.
- Casotto, C., Silva, V., Crowley, H., Nascimbene, R. and Pinho, R. (2015), "Seismic fragility of Italian RC precast industrial structures", *Eng. Struct.*, **94**, 122-136.
- CEN (2004), "Eurocode 8: Design of Structures for earthquake resistance", European Committee for Standardization, Brussels.
- Dassori, E. and Assobeton (2001), "La prefabbricazione in calcestruzzo: guida all'utilizzo nella progettazione", BE-MA.
- DPC (2016), Ran - Rete Accelerometrica Nazionale.
- Elliott, K. (2002), *Precast Concrete Structures*, Elsevier.
- Elliott, K.S. and Jolly, C. (2013), *Multi-Storey Precast Concrete Framed Structures*, Wiley.
- Elnashai, A.S. and Papazoglou, A.J. (1997), "Procedure and spectra for analysis of RC structures subjected to strong vertical earthquake loads", *J. Earthq. Eng.*, **1**(1), 121-155.
- Gülerçeç Z. and Abrahamson, N.A. (2011), "Site-specific design spectra for vertical ground motion", *Earthq. Spectra*, **27**(4),

- 1023-1047.
- Kramer, S.L. (1996), *Geotechnical Earthquake Engineering*, Pearson Education India.
- Liberatore, L., Sorrentino, L., Liberatore, D. and Decanini, L.D. (2013), "Failure of industrial structures induced by the Emilia (Italy) 2012 earthquakes", *Eng. Fail. Anal.*, **34**, 629-647.
- Lopez Garcia, D. and Soong, T.T. (2003a), "Sliding fragility of block-type non-structural components. Part 1: Unrestrained components", *Earthq. Eng. Struct. Dyn.*, **32**(1), 111-129.
- Lopez Garcia, D. and Soong, T.T. (2003b), "Sliding fragility of block-type non-structural components. Part 2: Restrained components", *Earthq. Eng. Struct. Dyn.*, **32**(1), 131-149.
- Magliulo, G., Capozzi, V., Fabbrocino, G. and Manfredi, G. (2011), "Neoprene-concrete friction relationships for seismic assessment of existing precast buildings", *Eng. Struct.*, **33**(2), 532-538.
- Magliulo, G., Ercolino, M., Petrone, C., Coppola, O. and Manfredi, G. (2014), "The Emilia earthquake: seismic performance of precast reinforced concrete buildings", *Earthq. Spectra*, **30**(2), 891-912.
- McKenna, F., Fenves, G.L., Scott, M.H. and Jeremic, B. (2013), "Open system for earthquake engineering simulation (OpenSees) [program]", Version 2.4.6, Pacific Earthquake Engineering Research Center, University of California at Berkeley, United States.
- MIT (2008), Ministerial Decree: NTC 2008-Norme tecniche per le costruzioni. (in Italian)
- Mohamad, M.E., Ibrahim, I.S., Abdullah, R., Rahman, A.B. Abd, Kueh, A.B.H. and Usman, J. (2015), "Friction and cohesion coefficients of composite concrete-to-concrete bond", *Cement Concrete Compos.*, **56**, 1-14.
- Newmark, N.M., Blume, J.A. and Kapur, K.K. (1973), "Seismic design spectra for nuclear power plants", Tech. Rept. Consulting Engineering Services, Urbana, IL.
- Pompei, A., Scalia, A. and Sumbatyan, M.A. (1998), "Dynamics of rigid block due to horizontal ground motion", *J. Eng. Mech.*, **124**(7), 713-717.
- Posada, M. and Wood, S. (2002), "Seismic performance of precast industrial buildings in Turkey", *7th US National Conference on Earthquake Engineering (7NCEE)*.
- Psycharis, I.N. and Mouzakis, H.P. (2012), "Assessment of the seismic design of precast frames with pinned connections from shaking table tests", *Bull. Earthq. Eng.*, **10**(6), 1795-1817.
- ReLUIs, ASSOBBETON, CNI and DPC (2012), "Linee di indirizzo per interventi locali e globali su edifici industriali monopiano non progettati con criteri antisismici", Available online at www.reluis.it.
- Sezen, H., Elwood, K.J., Whittaker, A.S., Mosalam, K.M., Wallace, J.W. and Stanton, J.F. (2000), "Structural engineering reconnaissance of the August 17, 1999 earthquake: Kocaeli (Izmit), Turkey", Pacific Earthquake Engineering Research Center.
- Taniguchi, T. (2002), "Non-linear response analyses of rectangular rigid bodies subjected to horizontal and vertical ground motion", *Earthq. Eng. Struct. Dyn.*, **31**(8), 1481-1500.
- Yenier, E., Erdoğan O. and Akkar, S. (2008), "Empirical relationships for magnitude and source-to-site distance conversions using recently compiled Turkish strong-ground motion database", *Proceedings of the 14th World Conference on Earthquake Engineering*.
- Zhu, J., Tan, P. and Jin, J. (2015), "Fragility analysis of existing precast industrial frames using CFRP reinforcement", *International Conference on Applied Science and Engineering Innovation (ASEI 2015)*.